ISSN 0006-3509, Biophysics, 2023, Vol. 68, No. 6, pp. 1004–1012. © Pleiades Publishing, Inc., 2023.
Russian Text © The Author(s), 2023, published in Biofizika, 2023, Vol. 68, No. 6, pp. 1210–1219.

BIOPHYSICS
OF COMPLEX SYSTEMS

The Dependence of the Oxygen Release Intensity from Erythrocytes on the Degree of Their Clustering in Sludges

I. A. Ponomarev[a,b] and G. Th. Guria[a,b,*]

[a] *National Medical Research Center for Hematology, Ministry of Health of the Russian Federation, Moscow, 125167 Russia*

[b] *Moscow Institute of Physics and Technology, Dolgoprudny, Moscow oblast, 141700 Russia*

**e-mail: guria@blood.ru*

Received April 26, 2023; revised April 26, 2023; accepted May 3, 2023

Abstract—An efficiency of oxygen release from red cells strongly depends on the regimes of their motion through microvessels. Mathematical model of oxygen transfer taking into account the red cells ability to form intravascular sludges has been constructed and studied. An analytical expression for the dependence of the oxygen release intensity on the size of erythrocyte sludges were derived. The possible significance of the obtained results for the express diagnostics of the red cell's ability for an oxygen transmission is discussed.

Keywords: oxygen transport function, erythrocyte sludge, oxygen release, erythrocyte parachute shape, erythrocyte clustering

DOI: 10.1134/S0006350923060167

INTRODUCTION

Erythrocytes are blood cells that play a key role in the transport of oxygen to organs and tissues. Hemoglobin acts as an oxygen carrier; it is a protein contained in erythrocytes that can exist in two forms, oxygenated and deoxygenated. Oxygen circulation in the human body includes the following stages: at the first stage, the formation of bonds between oxygen and hemoglobin molecules in the lungs takes place; at the second stage, the erythrocytes containing oxygenated hemoglobin are transferred with blood flow to organs and tissues; and the third stage is the release of oxygen from erythrocytes as a result of their deformation during movement in microvessels (capillaries) [1]. Modern methods of assessing the oxygen supply to the body, as a rule, are based on monitoring the first two stages in oxygen transport; they allow measuring the proportion of oxygenated hemoglobin contained in erythrocytes [2–4].

The issue of the amount of oxygen actually delivering to organs and tissues per unit of time has been taken into account only in some works [5–7]. Currently, this issue has become particularly relevant. The results of a number of studies indicate the "presence of problems" precisely at the third stage of oxygen transport [8–11]. It turned out that oxygenated hemoglobin can be contained in erythrocytes in sufficient quantities, however, when erythrocytes pass through microvessels, oxygen is not released from them [12, 13]. In such situations, with a normal level of blood saturation, patients show distinct signs of oxygen starvation (even asphyxia) [14, 15]. Finding out the causes of such effects has become especially relevant in connection with overcoming the consequences of COVID-19 pneumonia.

In this study, mathematical modeling methods were used to investigate the processes caused by changes in the shape of erythrocytes during their movement in microvessels. The focus was on the release of oxygen from deformed erythrocytes as they pass through the smallest vessels, microarterioles, and capillaries. Special attention has been paid to the processes of oxygen release from erythrocytes grouped into a sludges (intravascular aggregates of several erythrocytes [16, 17]).

It has been shown that the intensity of red blood cell oxygen release (heavily) decreases with the increasing of the sludge size. It was possible to obtain an explicit expression for the dependence of the intensity of oxygen release from erythrocytes on the degree of their clustering in sludge (see formula (12)). The prospects of creating a diagnostic method based on in vivo sludge detection are discussed, which will be operationally more informative than traditional in vitro methods used to assess the state of blood oxygen transport function.

Abbreviations: ESR, erythrocyte sedimentation reaction; COVID-19, coronavirus infection in 2019.

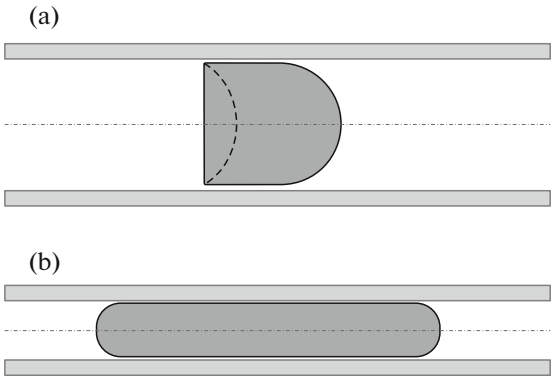

Fig. 1. Erythrocyte shapes when they are moving in microvessels: (a) parachute-like shape; and (b) an oblong shape, similar to a column.

FORMULATION OF THE PROBLEM

The movement of erythrocytes in microvessels that have a diameter smaller than the size of native erythrocytes in large vessels has been considered. The penetration of erythrocytes into microvessels, including capillaries, is associated with their deformation. The shape of erythrocytes moving in microvessels can significantly change depending on the volume of the erythrocyte (V), the surface of the membrane (S), and as the radius of the microvessel (R_c) [18, 19]. The movement of blood in large vessels is usually interpreted as the mass transfer of a homogeneous suspension consisting of plasma and cells (erythrocytes, platelets, etc.). In microvessels, heterogeneity plays an essential role in the dynamics of blood components, both individual and clustered erythrocytes (sludges) move under the action of forces acting on them from the plasma. In this work, it was assumed that erythrocytes are able to change their shape when moving in microvessels.

As is known, the change in the shape of the erythrocyte, its deformation (see Fig. 1), occurring in microvessels, is accompanied by oxygen desorption from hemoglobin molecules [20, 21]. Oxygen released as a result of erythrocyte deformation is able to diffuse through the erythrocyte membrane into the surrounding plasma. In this case, the rate of oxygen release from deformed erythrocytes is assumed to be directly proportional to the area of their membrane, which is directly in contact with blood plasma.

From qualitative considerations, it is clear that when there is clustering of individual erythrocytes in a sludge; the size of the membrane surface directly in contact with blood plasma is obviously less than the total surface of all erythrocytes included in the sludge. As a result, the intensity of oxygen release from erythrocytes entering the sludge should be less than from erythrocytes that can move separately in the capillaries.

The aim of the approach developed in this work was to find an explicit expression for the dependence of the intensity of oxygen release from erythrocytes on the degree of their clustering in sludge.

RESULTS

The Effect of Erythrocyte Shape in Microvessels on Oxygen Transport

The transport of free oxygen from the erythrocyte into the surrounding plasma is considered to occur due to passive diffusion. Because of this, the oxygen flow from the erythrocyte sludge (J) is assumed to be proportional to the product of the surface area of the sludge directly in contact with the blood plasma by the corresponding concentration difference:

$$J \propto \Delta C \Sigma, \tag{1}$$

where Σ is the surface area of the erythrocyte sludge and ΔC is the difference in oxygen concentrations inside the erythrocytes and in the sludge-washing plasma. It was assumed that erythrocytes, both in large vessels and in capillaries, have axial symmetry, and have a transverse circular cross section of radius r and length L. When moving in small vessels and capillaries, the anterior and posterior surfaces of erythrocytes have, generally speaking, a curvature is non-zero. However, first we consider the simplest cylindrical case (we will schematically consider the erythrocyte in the simplest "cylindrical" approximation), where L and r were considered to be related to the volume of an individual erythrocyte V and its surface S as follows:

$$S = 2\pi r^2 + 2\pi r L, \tag{2}$$

$$V = \pi r^2 L. \tag{3}$$

It is worth noting that the system of equations (2) and (3) for given values of V and S is ambiguously solvable with respect to the values of r and L. In fact, expressing the variable L from Eq. (2) and substituting the found expression into Eq. (3), we obtain a cubic equation:

$$V = \frac{1}{2} Sr - \pi r^3. \tag{4}$$

Equation (4) allows a graphical solution for the given values of V and S (see Fig. 2).

From Fig. 2 it can be seen that in cases where the volume of the erythrocyte V is less than some critical value V_* ($0 < V < V_*$), Eq. (4) admits two positive solutions r_1 and r_2. The value of V_* is determined by the following expression:

$$V_* = S^{3/2} \frac{1}{3\sqrt{6\pi}}. \tag{5}$$

The values of r_1 and r_2 are found according to the well-known formulas [22]:

$$r_1 = 2\sqrt[3]{\frac{V_*}{2\pi}}\cos((\varphi/3) - (2\pi/3)), \quad (6)$$

$$r_2 = 2\sqrt[3]{\frac{V_*}{2\pi}}\cos(\varphi/3), \quad (7)$$

where $\varphi = \arccos(-V/V_*)$. (Only two positive roots of Eq. (4) are given here. The negative root

$$r_3 = 2\sqrt[3]{\frac{V_*}{2\pi}}\cos((\varphi/3) + (2\pi/3))$$

does not make physical sense, since the radius cannot take negative values).

According to Eq. (4), the larger root $r = r_2$ corresponds to a shorter length $L_2 = V/\pi r_2^2$, and the smaller $r = r_1$ corresponds to a longer length $L_1 = V/\pi r_1^2$. A solution with a large radius ($r = r_2$) is associated with a "coin," and a solution with a smaller radius ($r = r_1$) is associated with a "column" (see Fig. 1b).

We note that the states of the erythrocyte in the form of a coin and a column differ in the energy required to deform the membrane. In fact, it is easy to find that the energy (E) associated with the curvature of the erythrocyte membrane is given by the following expression [23]:

$$E \sim \oiint_S \chi^2 dA \sim \left(\frac{1}{r}\right)^2 2\pi r L \sim \frac{L}{r} \sim \frac{1}{r^3}, \quad (8)$$

where χ denotes the local curvature of the erythrocyte membrane surface, and S denotes the complete surface of the erythrocyte.

Expression (8) shows that in the absence of steric restrictions, for a erythrocyte having a volume V and a surface area S it should be energetically more advantageous to be in a state with a large radius ($r = r_2$), that is, in the form of a coin, rather than in the form of an elongated column ($r = r_1$).

When penetrating into the microvessel under the influence of external forces, the erythrocyte is able to change its shape. If the radius of an erythrocyte in a column-type state turns out to be larger than the size of a microvessel, then for steric reasons such an erythrocyte is unable to penetrate into this microvessel. In other words, the necessary condition for the flow of erythrocytes with a given volume V and area S through a microvessel with a radius R_c has the form:

$$r_1(V, S) \le R_c, \quad (9)$$

where $r_1(V, S)$ is the smallest of the positive roots of Eq. (4), which is determined by Eq. (6).

If condition (9) is met, erythrocytes are able to pass through the capillary. At the same time, they can follow in the capillary both individually and like a train, interlocking in a sludge (see Appendix). Since the intensity of oxygen transport from each erythrocyte is determined by the fraction of the area of its membrane that is directly in contact with blood plasma, it is of interest to compare the regimes of piece-by-piece and sludge-clustered movement of erythrocytes in microvessels.

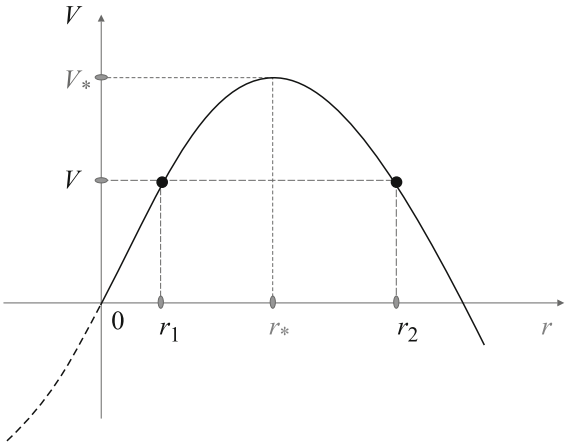

Fig. 2. The cubic curve corresponds to the right side of Eq. (4), where r is the radius of the erythrocyte, V is the volume of the erythrocyte; V_* and r_* are critical values of the volume and radius; r_1 and r_2 are two values of radius that the erythrocyte can have at volume V. For $V > V_*$, Eq. (4) has no solutions for $r > 0$. There are two solutions for $V < V_*$. The first of them (r_1) corresponds to the case of a column. The second solution (r_2) corresponds to the coin case.

It is easy to show that in the considered cylindrical approximation, the plasma-contacting surface of each erythrocytes is given by the following expression:

$$\Sigma_1 = 2\pi r_1^2 + 2\pi r_1 L_1. \quad (10)$$

At the same time, for N erythrocytes passing through the capillary as part of a sludge, the total value surface in contact with plasma is given by the expression:

$$\Sigma_N = 2\pi r_1^2 + N 2\pi r_1 L_1. \quad (11)$$

When condition (9) is fulfilled, it is not difficult to obtain from expressions (10) and (11) the ratio of the oxygen flow J_N from a sludge containing N erythrocytes to the total flow from N erythrocytes moving alone in the capillary:

$$\frac{J_N}{NJ_1} = \frac{\varepsilon}{\varepsilon + 1} + \left(\frac{1}{\varepsilon + 1}\right)\frac{1}{N}, \quad (12)$$

where J_1 indicates the oxygen flow from the sequestered erythrocyte. For the value ε is used the designation:

$$\varepsilon = L_1/r_1. \quad (13)$$

Since $r_1(V, S) \le R_c$, to obtain majority estimates, the ε parameter was calculated at $r_1 = R_c$.

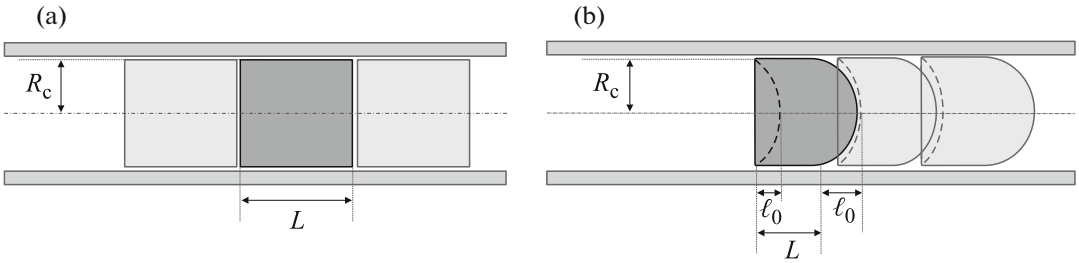

Fig. 3. A schematic representation of erythrocytes in a microvessel, where R_c is the radius of the microvessel; L is the length of the erythrocyte sludge: (a) simple cylindrical approximation; (b) cylindrical approximation with the approximation of the anterior and posterior ends with spherical segments, where ℓ_0 is the height of the spherical segment.

The resulting expression (12) shows that when cylindrical approximation of erythrocytes is used (see Fig. 3a), the intensity of oxygen release from the erythrocyte should decrease inversely in proportion to the size of the sludge (N), which includes this erythrocyte.

It should be noted that expression (12) was obtained assuming that the front and rear cylindrical ends are flat. In this regard, it seemed necessary to study the effect of curvature of the anterior and posterior parts of erythrocytes on the intensity of oxygen release from erythrocytes when they are squeezed through microvessels. Erythrocytes with rounded anterior and posterior parts are often observed in experiments [24–26]. At the same time, in erythrocytes with a parachute-like shape, the front part is usually convex, and the back is concave (see Fig. 3b).

It turned out (see Appendix) that even when taking the curvature of the anterior and posterior surfaces into account, the ratio of the oxygen flow from the sludge to the total flow from the same number of sequestered erythrocytes is given by an expression similar to Eq. (12), in which the parameter ε appears instead of the parameter $\tilde{\varepsilon}$. The value of the parameter $\tilde{\varepsilon}$ when approximating the anterior and posterior ends of erythrocytes with spherical segments (see Fig. 3b) is easily found:

$$\tilde{\varepsilon} = \varepsilon/\left(1 + \tilde{\ell}_0^2\right), \tag{14}$$

where $\tilde{\ell}_0 = \ell_0/R_c$ and $\tilde{\ell}_0$ is the ratio of the height of the spherical segment to the radius of the vessel R_c (Fig. 3b).

In addition to the shape of erythrocytes, approximated using spherical convex-concave end segments, several other options were considered. Considering the geometric features of the curvature of the anterior and posterior surfaces, it turned out that in all the cases we considered, the ratio of the oxygen flow from the sludge to the total flow from the corresponding number of isolated erythrocytes is given by an expression of type (12), in which the properly modified value ε appears as the parameter $\tilde{\varepsilon}$ (see Appendix).

DISCUSSION

As far as the authors know, the dependence of the intensity of oxygen release on the size of sludge has not been analyzed theoretically to date. The formula (12) obtained in this study, with a number of simplifying assumptions, initially seemed insufficiently robust. However, the analysis carried out for a number of realistic forms of erythrocytes showed that the relationship between the intensity of oxygen release from erythrocytes entering the sludge and the size of the sludge in all considered cases is given by expressions isomorphic to expression (12) in their mathematical structure (see Appendix). It turned out that the values representing the ratio of the effective length of the erythrocyte (taking the curvature of its ends into account) to the radius of the microvessel appear as the parameter ε. In this sense, by its structure, expression (12) obtained in this study seems, if not universal, then rather general.

When describing the release of oxygen from erythrocytes, for the sake of simplicity, we assumed this process to be limited by diffusion (see formula (1)). The contribution of the effects associated with the release of water from deformable erythrocytes was clearly not considered. However, such effects on the filterability of erythrocytes through microvessels can, in principle, make a certain contribution to oxygen transport. To analyze the effects associated with the release of water and oxygen dissolved in it from erythrocytes, it is necessary to correct expression (1) by adding a convective term to its right side:

$$J \propto (D\Delta C + vC)\Sigma, \tag{15}$$

where Σ is the surface area of the erythrocyte sludge in direct contact with plasma; ΔC is the difference in oxygen concentrations inside erythrocytes and in the sludge-washing plasma; D is the oxygen diffusion coefficient; C is the oxygen concentration; and v is the rate of water exit through the erythrocyte membrane.

A comparison of expressions (1) and (15) shows that in both cases, the surface area of erythrocytes (Σ) in direct contact with blood plasma is multiplicatively included in both expressions. This means that with additional consideration of the effects associated with the release of water from erythrocytes the overall

decrease in the surface during their clustering in sludge has exactly the same effect on the intensity of oxygen release as in the case of diffusion transport only. In other words, expression (12) and its analogues (see Appendix) should also remain valid when considering the convective mass transfer of oxygen through the erythrocyte membrane during their movement in microvessels.

The question of the conditions under which erythrocytes moving in microvessels are capable of aggregation into a sludge requires further study. Currently, the erythrocyte sedimentation reaction (ESR) is widely used for diagnostic purposes, which displays the rate of erythrocyte sedimentation in whole donor blood in vitro. Studies have shown that the erythrocyte sedimentation reaction in whole blood in vitro is of a two-phase nature. It begins with the first rapid phase of the formation of macroscopically extended coin columns consisting of aggregated erythrocytes [27, 28]. The first phase is followed by a second, slow phase, the destruction of these columns in the gravity field, which leads to the fractionation of blood into a concentrate of erythrocytes and plasma over it. According to the rate of movement of the boundary of a concentrate of erythrocytes and plasma during fractionation of whole blood in the field of gravity, it is customary to judge the degree of development of pathological conditions.

In this regard, it seems that the phenomenon of clustering of erythrocytes in microvessels is naturally interpreted as the initial phase of the formation of coin columns under in vivo conditions [29]. If this assumption is correct, then methods for recording the processes of sludge formation in vivo should be of no less diagnostic value for practical purposes than ESR test in vitro. It follows from the results obtained in this work that the average value of the sludge may be of interest not only as a measure that operationally characterizes the rate of reactions of the coin formation columns in in vivo conditions, but also as an indicator that significantly determines the level of decrease in the intensity of oxygen release from erythrocytes. In fact, it follows from formula (12) that information on the time change in the average degree of erythrocyte aggregation during their squeezing through microvessels can be used to assess the decrease in the intensity of oxygen release from erythrocytes.

A decrease in effective oxygen transport function is one of the undesirable consequences of the effects caused by the aggregation of erythrocytes in the bloodstream. The physiological and pathological effects on the human body leading to the appearance of sludge were studied in detail in [30–32], including using capillaroscopy with optical methods [33, 34]. The attractiveness of sludge detection methods in in vivo systems is determined by the simplicity and efficiency of their implementation [35, 36]. It takes minutes to perform these tests, instead of hours, as in the case of ESR. Detection of an increased degree of erythrocyte aggregation in microvessels can be considered as an early indicator of the development of undesirable pathologies. In this regard, the expressions (12) and (13) obtained in this work allow us to judge the degree of severity of violations of oxygen transport function in the body by the average size of the sludge moving in the microvessels.

It can be assumed that the use of techniques for in vivo sludge detection will make it possible to create in the future a diagnostic method that is operationally more informative than the traditionally used methods in vitro based on the ESR test.

APPENDIX

The Effect of Curvature of the Ends of Erythrocytes on the Intensity of Oxygen Release

The conducted study allowed us to obtain a simple expression (12) for the intensity of oxygen release from erythrocyte sludge. However, the question remains unresolved: is expression (12) valid beyond the assumptions used in the main text of the work?

This appendix is devoted to the analysis of the effect of the shape of erythrocytes with curved ends on the process of oxygen release from erythrocytes included in the sludge. The forms that allow dense packing of erythrocytes in sludges were considered.

The Intensity of Oxygen Release from Erythrocytes after Taking the Spherical Curvature of Both Ends into Account

When taking the curvature of the ends of parachute-shaped erythrocytes into account, the latter were considered to have spherical segments located at the anterior and posterior ends (see Fig. 4).

In this case, the system of equations (2) and (3) takes the form:

$$V = \pi R_c^2 L, \tag{A1}$$

$$S = 2\pi\left(R_c^2 + \ell_0^2\right) + 2\pi R_c L. \tag{A2}$$

Expressions (A1) and (A2) after de-dimensioning take the form:

$$\tilde{V} = \varepsilon, \tag{A3}$$

$$\tilde{S} = 2\left[1 + \left(\tilde{\ell}_0\right)^2 + \varepsilon\right], \tag{A4}$$

where the used designations are:

$$\begin{aligned} \varepsilon &= L/R_c, \\ \tilde{S} &= S/\left(\pi R_c^2\right), \\ \tilde{V} &= V/\left(\pi R_c^3\right), \\ \tilde{\ell}_0 &= \ell_0/R_c. \end{aligned} \tag{A5}$$

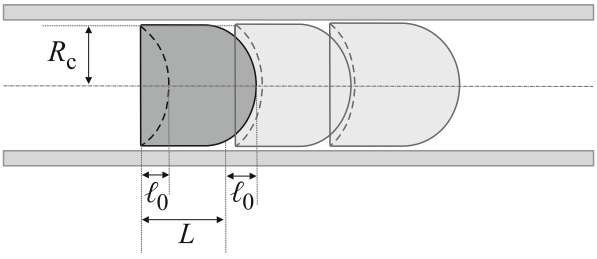

Fig. 4. A schematic representation of an erythrocyte in a cylindrical approximation with both ends of spherical shape. A lateral projection of the cell is presented with the designation of the values used in the consideration, where L is the length of the cylindrical part of the erythrocyte, R_c is the inner radius of the capillary, ℓ_0 is the height of the spherical segment (in the considered case, the radius of curvature of the end of spherical shape (R) is given by the expression $R = (R_c^2 + \ell_0^2)/2\ell_0$.

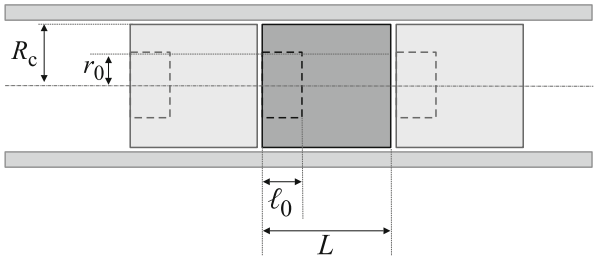

Fig. 5. An illustration of the erythrocyte in a cylindrical approximation, taking the curvature of the posterior end into account. A lateral projection of the cell is presented with the designation of the values used in the consideration, where L is the length of the cylindrical part of the erythrocyte, R_c is the inner radius of the capillary, ℓ_0 is the height of the cylindrical cutout; r_0 is the radius of the cylindrical cutout in the rear end.

Solving the system of equations (A3) and (A4), we obtain the expression for $\tilde{\ell}_0$:

$$\tilde{\ell}_0 = \sqrt{\frac{\tilde{S}}{2} - \varepsilon - 1}. \quad \text{(A6)}$$

Using the expression (A6) for the ratio of oxygen release from the erythrocytes included in the sludge, compared with the separately moving erythrocytes, it is easy to obtain the expression:

$$\frac{J_N}{NJ_1} = \frac{2\pi\left(R_c^2 + \ell_0^2\right) + 2\pi NR_cL}{2N\pi\left(R_c^2 + \ell_0^2\right) + 2\pi NR_cL} = \frac{1 + \left(\tilde{\ell}_0\right)^2 + N\varepsilon}{N\left[1 + \left(\tilde{\ell}_0\right)^2\right] + N\varepsilon} = \frac{\varepsilon}{1 + \left(\tilde{\ell}_0\right)^2 + \varepsilon} + \frac{1 + \left(\tilde{\ell}_0\right)^2}{1 + \left(\tilde{\ell}_0\right)^2 + \varepsilon}\frac{1}{N}, \quad \text{(A7)}$$

where J_N is the oxygen flow from the erythrocytes entering the sludge; J_1 is the oxygen flow from the erythrocyte moving separately; and N is the number of erythrocytes entering the sludge; expressions for the parameters are presented in the formula (A5).

Equation (A7), using the designation $\tilde{\varepsilon} = \varepsilon/\left[1 + (\tilde{\ell}_0)^2\right]$, is easily reduced to the form

$$\frac{J_N}{NJ_1} = \frac{\tilde{\varepsilon}}{1 + \tilde{\varepsilon}} + \frac{1}{1 + \tilde{\varepsilon}}\frac{1}{N}. \quad \text{(A8)}$$

If we compare expression (A8) with expression (12) of the main text, it can be seen that taking the shape of erythrocytes with ends in the form of spherical segments into account leads to exactly the same kind of dependence of the intensity of oxygen release from erythrocytes on the size of the erythrocyte sludge. In this case, the value of the $\tilde{\varepsilon}$ parameter is given by the expression

$$\tilde{\varepsilon} = \varepsilon/\left(1 + \left(\tilde{\ell}_0\right)^2\right),$$

where $\tilde{\ell}_0$ characterizes the height of the spherical segments at the ends.

Oxygen Release from Erythrocytes after Taking the Piecewise Curved Posterior End into Account

The curvature of the ends of parachute-shaped erythrocytes can be approximated not only by using a spherical approximation. In this section of the Appendix, we will consider how the expression should look for the intensity of oxygen release from erythrocytes, whose shape is represented by a cylinder with a cylindrical cutout in the rear end (see Fig. 5).

For the erythrocyte volume, the valid expression is:

$$V = \pi R_c^2 L - \ell_0 \pi r_0^2. \quad \text{(A9)}$$

The surface area of the erythrocyte is determined by the formula:

$$S = 2\pi R_c^2 L + 2\pi R_c L + 2\pi r_0 \ell_0. \quad \text{(A10)}$$

De-dimensioning equations (A9) and (A10) by replacing (A5) and $\tilde{r}_0 = r_0/R_c$ gives:

$$\tilde{V} = \varepsilon - \tilde{\ell}_0 \tilde{r}_0^2, \quad \text{(A11)}$$

$$\frac{\tilde{S}}{2} = 1 + \varepsilon + \tilde{\ell}_0 \tilde{r}_0. \quad \text{(A12)}$$

The solution of the system (A11)–(A12) allows finding expressions for $\tilde{\ell}_0$ and $\tilde{r}_0$:

$$\tilde{\ell}_0 = \frac{\left(\frac{\tilde{S}}{2} - 1 - \varepsilon\right)^2}{\varepsilon - \tilde{V}}, \quad \text{(A13)}$$

$$\tilde{r}_0 = \frac{\varepsilon - \tilde{V}}{\frac{\tilde{S}}{2} - 1 - \varepsilon}. \quad \text{(A14)}$$

It is easy to show that with this type of approximation $\varepsilon - \tilde{V} \geq 0$. Using expressions (A13) and (A14) for the ratio of oxygen release from erythrocytes entering the sludge, compared with separately moving erythrocytes, it is easy to obtain the following expression:

$$\frac{J_N}{NJ_1} = \frac{2\pi R_c^2 + 2\pi r_0 \ell_0 + 2\pi N R_c L}{2\pi N R_c^2 + 2\pi N r_0 \ell_0 + 2\pi N R_c L} = \frac{1 + \tilde{\ell}_0 \tilde{r}_0 + N\varepsilon}{N + N\tilde{\ell}_0 \tilde{r}_0 + N\varepsilon} = \frac{\varepsilon}{1 + \tilde{\ell}_0 \tilde{r}_0 + \varepsilon} + \frac{1 + \tilde{\ell}_0 \tilde{r}_0}{1 + \tilde{\ell}_0 \tilde{r}_0 + \varepsilon} \frac{1}{N}, \quad \text{(A15)}$$

where J_N is the oxygen flow from the erythrocytes entering the sludge; J_1 is the oxygen flow from the erythrocyte moving separately; N is the number of erythrocytes entering the sludge; $\tilde{r}_0 = r_0/R_c$, and the expressions for the remaining parameters are presented in formula (A5).

Equation (A15) is reduced to the form

$$\frac{J_N}{NJ_1} = \frac{\tilde{\varepsilon}}{1 + \tilde{\varepsilon}} + \frac{1}{1 + \tilde{\varepsilon}} \frac{1}{N}, \quad \text{(A16)}$$

where

$$\tilde{\varepsilon} = \varepsilon / \left(1 + \tilde{\ell}_0 \tilde{r}_0\right)$$

A comparison of expression (A16) with expression (12) of the main text shows that taking the piecewise linear curvature of the shape of the posterior end of erythrocytes into account leads to exactly the same type of dependence of the intensity of oxygen release from erythrocytes on the size of the erythrocyte sludge. In this case, the value of the $\tilde{\varepsilon}$ parameter is given by the expression

$$\tilde{\varepsilon} = \varepsilon / \left(1 + \tilde{\ell}_0 \tilde{r}_0\right),$$

where $\tilde{\ell}_0 \tilde{r}_0$ characterizes the curvature of the posterior end of the erythrocyte.

The Release of Oxygen from Erythrocytes, Described after Taking the Piecewise Linear Curvature of the Anterior and Posterior Ends into Account

The curvature of the ends of parachute-shaped erythrocytes can be taken into account not only in the approximations described above. In this section of the appendix, we will consider how the expression should look for the intensity of oxygen release from erythrocytes, whose shape is represented by a cylinder with a cutout in the rear end and a cylindrical bulge in the front (see Fig. 6).

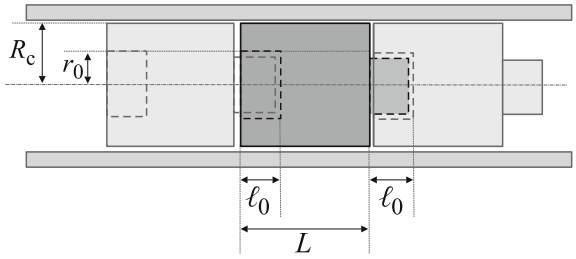

Fig. 6. An illustration of the erythrocyte in a cylindrical approximation taking into account the curvature of the anterior and posterior ends. A lateral projection of the cell is presented with the designation of the values used in the consideration, where L is the length of the cylindrical part of the erythrocyte, R_c is the inner radius of the capillary, ℓ_0 is the height of the cylindrical cutout and bulge; r_0 is the radius of the cylindrical cutout in the rear end and the bulge in the front.

The volume and surface area of erythrocytes are given by expressions:

$$V = \pi R_c^2 L, \quad \text{(A17)}$$

$$S = 2\pi R_c^2 + 2\pi R_c L + 4\pi r_0 \ell_0. \quad \text{(A18)}$$

By de-dimensioning equations (A9) and (A10) we obtain:

$$\tilde{V} = \varepsilon, \quad \text{(A19)}$$

$$\frac{\tilde{S}}{2} = 1 + \varepsilon + \tilde{\ell}_0 \tilde{r}_0, \quad \text{(A20)}$$

where substitutions (A5) and $\tilde{r}_0 = r_0/R_c$ are introduced.

From Eq. (A20) for $\tilde{\ell}_0 \tilde{r}_0$ we obtain the following expression:

$$\tilde{\ell}_0 \tilde{r}_0 = \frac{\tilde{S}}{2} - 1 - \varepsilon. \quad \text{(A21)}$$

By virtue of expressions (1) and (14), the intensity of oxygen release is proportional to the surface area of the erythrocyte sludge in direct contact with the surrounding plasma. Using the expression (A21) for the ratio of oxygen release from erythrocytes included in the sludge, compared with separately moving erythrocytes, it is easy to obtain the following expression:

$$\frac{J_N}{NJ_1} = \frac{2\pi R_c^2 + 4\pi r_0 \ell_0 + 2\pi N R_c L}{2\pi N R_c^2 + 4\pi N r_0 \ell_0 + 2\pi N R_c L} = \frac{1 + 2\tilde{\ell}_0 \tilde{r}_0 + N\varepsilon}{N + 2N\tilde{\ell}_0 \tilde{r}_0 + N\varepsilon} = \frac{\varepsilon}{1 + 2\tilde{\ell}_0 \tilde{r}_0 + \varepsilon} + \frac{1 + 2\tilde{\ell}_0 \tilde{r}_0}{1 + 2\tilde{\ell}_0 \tilde{r}_0 + \varepsilon} \frac{1}{N}, \quad \text{(A22)}$$

where J_N is the oxygen flow from the erythrocytes entering the sludge; J_1 is the oxygen flow from the erythrocyte moving separately and N is the number of

erythrocytes entering the sludge; $\tilde{r}_0 = r_0/R_c$, the expressions for the remaining parameters are presented in the formula (A5).

Equation (A22) is reduced to the form

$$\frac{J_N}{NJ_1} = \frac{\tilde{\varepsilon}}{1+\tilde{\varepsilon}} + \frac{1}{1+\tilde{\varepsilon}}\frac{1}{N}, \quad \text{(A23)}$$

where

$$\tilde{\varepsilon} = \varepsilon/\left(1 + 2\tilde{\ell}_0\tilde{r}_0\right).$$

The expression (A21) is valid for the value $\tilde{\ell}_0\tilde{r}_0$. If we compare expression (A23) with expression (12) of the main text, it can be seen that taking the piecewise linear curvature of the shape of the anterior and posterior ends of erythrocytes into account leads to exactly the same kind of dependence of the intensity of oxygen release from erythrocytes on the size of the erythrocyte sludge. In both cases, the hyperbolic nature of this dependence takes place. In this case, the value of the $\tilde{\varepsilon}$ parameter is given by the expression

$$\tilde{\varepsilon} = \varepsilon/\left(1 + 2\tilde{\ell}_0\tilde{r}_0\right),$$

where $\tilde{\ell}_0\tilde{r}_0$ characterizes the curvature of the posterior end of the erythrocyte.

The Structural Invariance of the Expression for Oxygen Release from Erythrocyte Sludge

The value of $\tilde{\varepsilon}$ for arbitrarily complex shapes of the end sections of erythrocytes can be calculated using the Archimedes exhaustion method. The method consists of dividing the complex geometric structure of the ends into elementary cylindrical segments, "pancakes." Such decompositions into elementary pancakes make it possible to find the upper and lower Darboux sums. The intensity of oxygen release is "squeezed" between the upper and lower Darboux sums and can be calculated using the lemma about "two policemen" by limiting the transition. The analysis of cylindrical erythrocytes with pancakes attached to them is described in the appendix, according to the authors of this work, suggests that even in the case of curvature of the "general position" the structure of the equations describing the intensity of oxygen release will not change. These considerations support the invariance of the structure of Eq. (12).

ACKNOWLEDGMENTS

The work was performed at the NMRC of Hematology of the Ministry of Health of the Russian Federation. The authors thank the staff of the Laboratory of Mathematical Modeling of biological processes for fruitful discussions and valuable comments.

FUNDING

This work was supported by ongoing institutional funding. No additional grants to carry out or direct this particular research were obtained.

ETHICS APPROVAL AND CONSENT TO PARTICIPATE

This work does not contain any studies involving human and animal subjects.

CONFLICT OF INTEREST

The authors of this work declare that they have no conflicts of interest.

REFERENCES

1. C. Wang and A. S. Popel, Math. Biosci. **116** (1), 89 (1993). https://doi.org/10.1016/0025-5564(93)90062-f
2. E. Ortiz-Prado, J. F. Dunn, J. Vasconez, et al., Am. J. Blood Res. **9**, 1 (2019).
3. A. Sircan-Kucuksayan, M. Uyuklu, and M. Canpolat, Physiol. Meas. **36**, 2461 (2015). https://doi.org/10.1088/0967-3334/36/12/2461
4. A. M. Pilotto, A. Adami, R. Mazzolari, et al., J. Physiol. **600**, 4153 (2022). https://doi.org/10.1113/JP283267
5. N. Tateishi, N. Maeda, and T. Shiga, Circ. Res. **70** (4), 812 (1992). https://doi.org/10.1161/01.RES.70.4.812
6. A. G. Tsai, P. C. Johnson, and M. Intaglietta, Physiol. Rev. **83**, 933 (2003). https://doi.org/10.1152/physrev.00034.2002
7. D. C. Poole, T. I. Musch, and T. D. Colburn, Eur. J. Appl. Physiol. **122**, 7 (2022). https://doi.org/10.1007/s00421-021-04854-7
8. H. Kohzuki, S. Sakata, Y. Ohga, et al., Jpn. J. Physiol. **50**, 167 (2000). https://doi.org/10.2170/jjphysiol.50.167
9. N. Tateishi, Y. Suzuki, I. Cicha, and N. Maeda, Am. J. Physiol., Heart Circ. Physiol. **281**, H448 (2001). https://doi.org/10.1152/ajpheart.2001.281.1.H448
10. M. Uyuklu, H. J. Meiselman, and O. K. Baskurt, Clin. Hemorheol. Microcirc. **41**, 179 (2009). https://doi.org/10.3233/CH-2009-1168
11. A. Semenov, A. Lugovtsov, P. Ermolinskiy, et al., Photonics **9**, 238 (2022). https://doi.org/10.3390/photonics9040238
12. R. J. Tomanek, Anatom. Record **305**, 3199 (2022). https://doi.org/10.1002/ar.24951
13. D. C. Poole and T. I. Musch, Function **4**, zqad013 (2023). https://doi.org/10.1093/function/zqad013
14. A. Melkumyants, L. Buryachkovskaya, N. Lomakin, et al., Thromb. Haemostasis **122**, 123 (2022). https://doi.org/10.1055/a-1551-9911

15. A. Gupta, M. V. Madhavan, K. Sehgal, et al., Nat. Med. **26**, 1017 (2020). https://doi.org/10.1038/s41591-020-0968-3
16. S. Chien, *The Red Blood Cell*, Ed. by D. M. Surgenor (Academic, London, 1975), pp. 1031–1133.
17. A. N. Beris, J. S. Horner, S. Jariwala, et al., Soft Matter **17**, 10591 (2021). https://doi.org/10.1039/D1SM01212F
18. D. A. Fedosov, M. Peltomaki, and G. Gompper, Soft Matter **10**, 4258 (2014). https://doi.org/10.1039/C4SM00248B
19. N. Z. Piety, W. H. Reinhart, P. H. Pourreau, et al., Transfusion **56**, 844 (2016). https://doi.org/10.1111/trf.13449
20. T. J. McMahon, Front. Physiol. **10**, 1417 (2019). https://doi.org/10.3389/fphys.2019.01417
21. J. T. Celaya-Alcala, G. V. Lee, A. F. Smith, et al., J. Cereb. Blood Flow Metab. **41** (3), 656 (2021). https://doi.org/10.1177/0271678X20927100
22. I. N. Bronshtein, K. A. Semendyaev, *Handbook of Mathematics for Engineers and College Students* (Toibner, Leiptsig, 1981; Nauka, Moscow, 1981), pp. 169–170.
23. P. B. Canham, J. Theor. Biol. **26**, 61 (1970). https://doi.org/10.1016/S0022-5193(70)80032-7
24. T. Shiga, N. Maeda, and K. Kon, Crit. Rev. Oncol. / Hematol. **10** (1), 9 (1990). https://doi.org/10.1016/1040-8428(90)90020-S
25. T. Tajikawa, Y. Imamura, T. Ohno, et al., J. Biorheol. **27**, 1 (2013). https://doi.org/10.1007/s12573-012-0052-9
26. T. W. Secomb, Annu. Rev. Fluid Mech. **49**, 443 (2017). https://doi.org/10.1146/annurev-fluid-010816-060302
27. V. L. Voeikov, Usp. Fiziol. Nauk **29**, 55 (1998).
28. A. Rabe, A. Kihm, A. Darras, et al., Biomolecules **11**, 727 (2021). https://doi.org/10.3390/biom11050727
29. Yu. I. Gurfinkel, O. A. Korol, and G. E. Kufal, Proc. SPIE, **3260**, 232 (1998). https://doi.org/10.1117/12.307096
30. I. Cicha, Y. Suzuki, N. Tateishi, and N. Maeda, Am. J. Physiol., Heart Circ. Physiol. **284**, H2335 (2003). https://doi.org/10.1152/ajpheart.01030.2002
31. Y. Arbel, S. Banai, J. Benhorin, et al., Int. J. Cardiol. **154**, 322 (2012). https://doi.org/10.1016/j.ijcard.2011.06.116
32. M. A. Elblbesy and M. E. Moustafa, Int. J. Biomed. Sci. **13**, 113 (2017).
33. R. N. Pittman, Microcirculation **20**, 117 (2013). https://doi.org/10.1111/micc.12017
34. A. E. Lugovtsov, Y. I. Gurfinkel, P. B. Ermolinskiy, et al., *Biomedical Photonics for Diabetes Research*, Ed. by A. V. Dunaev and V. V. Tuchin (CRC, London, 2023), pp. 57–79. https://doi.org/10.1201/9781003112099
35. E. Hysi, R. K. Saha, and M. C. Kolios, J. Biomed. Opt. **17**, 125006 (2012). https://doi.org/10.1117/1.JBO.17.12.125006
36. T. H. Bok, E. Hysi, and M. C. Kolios, Biomed. Opt. Express **7**, 2769 (2016). https://doi.org/10.1364/BOE.7.002769

Translated by E. Puchkov